Chapter 4
Positive Temperature Coefficient Effect of Polymer Nanocomposites

Haiping Xu

4.1 Introduction

Positive temperature coefficient (PTC) of resistivity is an interesting phenomenon in the field of conductive polymer nanocomposites (CPC) consisting of an insulating polymer matrix and conductive fillers, which change their resistivity at the critical temperature by several orders of magnitude. Because of the commercial significance of such a temperature-activated switching feature, the PTC nanocomposites can be utilized in a wide range of industrial applications, such as self-regulating heaters, current protection devices, microswitch sensors, and other outdoor equipments [1–7]. Polymer-based PTC nanocomposites have been paid more attention because of the advantages of excellent formability, flexibility, and lightweight over the conventional inorganic PTC materials, though they have some shortcomings, such as unstable electrical reproducibility and negative temperature coefficient (NTC) effect phenomena when above the melting temperature of polymers.

Polymer materials incorporated with conductive fillers exhibiting the PTC effect were first discovered by Frydman in a carbon black (CB)-filled low-density polyethylene (LDPE) composite in 1945 [8]. After that, the PTC phenomenon has attracted much interest and studies [9–14], and the mechanism of PTC effect for CPC is also turned into the focus of the study.

In this chapter, several theories as well as their characteristics in polymer PTC nanocomposites are summarized. The key factors that influence the PTC properties such as matrix, kinds of fillers, constructural composition, and process technologies are analyzed.

H. Xu, PhD (✉)
Department of Material Engineering, School of Environmental and Materials Engineering
College of Engineering, Shanghai Second Polytechnic University, Shanghai 201209, China
e-mail: hpxu@sspu.edu.cn

X. Huang, C. Zhi (eds.), *Polymer Nanocomposites*,
DOI 10.1007/978-3-319-28238-1_4

4.2 Conduction Mechanism of CPC

The conductivity of CPC depends critically on the filler volume content f [15]. The conductivity increases as

$$\rho(f) \propto (f - f_c)^{-t} \tag{4.1}$$

with a parameter t between 1.65 and 2 for three-dimensional lattices [16]. f_c is called the critical or percolation threshold. The percolation behavior can be influenced by the shape of fillers. For random packing in three dimensions, f_c turns out to be about 16 %.

Figure 4.1 schematically illustrates the percolation curve of resistivity and the cluster structures of fillers, based on reports by Nakamura et al. [17]. When f is in region I, the resistivity of nanocomposite nearly equals that of the insulating polymer. At a critical filler content, f_c, in region II, the resistivity is dominated by tunneling conduction of electrons between clusters because gaps now exist between the fillers. In contrast, when the filler content is above f_c, in region III, the tunneling

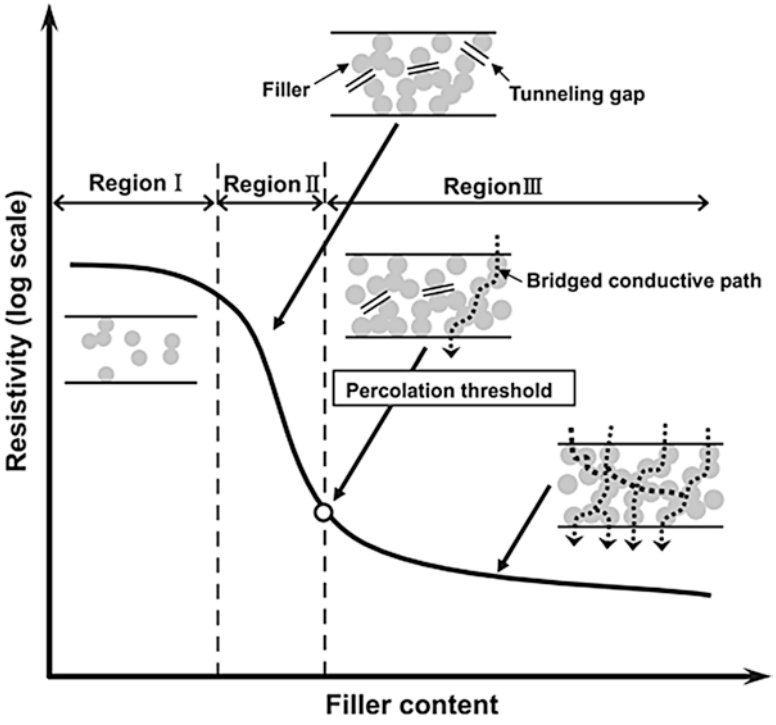

Fig. 4.1 Schematic of the general percolation curve and the presumptive cluster structure of conductive fillers (Reprinted with permission from Ref. [17]. Copyright 2012 Elsevier Ltd.)

gaps between clusters are destroyed by increasing filler content, and an ohmic conductive path is generated due to the bridged cluster between electrodes.

4.3 Theoretical and Phenomenological Background of PTC Effect

It is generally believed that the PTC effect is caused by a breakup of conductive network during sample heating. Several theories have been proposed to elucidate the specific nonlinear shift in resistivity with temperature parameter, such as thermal expansion, electron tunnel effect, electrical field emission, as well as the inner stress and phonon-assisted tunneling models. Nevertheless, these theories still remain in some problems and cannot explain experimental results clearly.

4.3.1 Conducting Chain and Thermal Expansion Theory

Kohler first suggested in 1961 that the PTC mechanism was a function of difference in thermal expansion coefficients between matrix and filler [18]. The sudden expansion, which took place at the melting point of the polymer matrix, resulted in the breakup of the conducting chains with a consequent anomalous increase in the resistivity. However, this model was not able to explain the steep decrease in resistivity above melting temperature (T_m) (so-called NTC effect), when the volume of matrix continued to increase with temperature.

4.3.2 Tunneling Current Mechanism

In contrast, the model proposed by Ohe and Natio assumed that a more uniform distribution of interparticle gaps and the gap width is small enough to allow intensive tunneling to take place at a low temperature [19]. The distribution of gaps became more random at temperatures near T_m, and a significant number of interparticle gaps were too large to allow appreciable electron tunneling, although the average gap width did not change considerably. This resulted in the elimination of many conductive paths with a consequent rise in resistivity. The influence of matrix on the PTC effect and increasing randomness of the interparticle gaps as T_m was approached were unexplained. The NTC effect, which usually took place immediately above the melting point of the matrix, also remained unexplained.

The tunneling model was further modified by Meyer taking the effect of change in crystallinity into consideration [20]. Meyer proposed the conductive particles existing only in amorphous regions being separated by crystalline films, which has

been assumed to be more conductive than amorphous ones. Thus he suggested that the anomalous rise in resistivity near melting point can be attributed to the melting of crystals. He also proposed that the NTC effect might be attributed to the immigration of CB particles, which resulted in the formation of new conductive chains of the filler particles.

Although Meyer's model can explain PTC and NTC phenomena, he has not referred to the effect of crystalline change and the NTC effect.

4.3.3 Mechanism of Congregation and Migration Changes of Filler Particles

Klason et al. explained the PTC and NTC effects on the basis of changes taking place in the carbon congregation structure with temperature [21]. Although they suggested that the NTC effect was due to the formation of new networks of conductive particles, this process was not explained in detail. On the other hand, Voet et al. attributed the PTC effect to the large volume expansion of the polymer in melting range, as well as the migration of CB to the previously CB-free crystalline region as mentioned above, which further diluted the concentration of the filler in matrix and increased resistivity [22].

4.3.4 Electrical Field Emission Mechanism

Based on above viewpoints, Allak H. K. proposed that contact resistance between particles is important in case that filler volume concentration exceeds the percolation threshold, and charge transport through filler phase takes place via direct contact between particles. On the contrary, when a thin, insulating polymer layer separates the filler particles, conductivity is dominated by charge transport via tunneling effect [23].

Additionally, the dynamic factor resulting in reaggregation of CB particles has been considered as the attraction between them (such as Van der Waals interaction or covalent bonds between them), which is too weak to overcome the separation resulting from vigorous macromolecular movement at temperatures over T_m, so NTC effect is caused by a decrease of elastic modules of polymer at high temperature.

4.3.5 Internal Stress Mechanism

During curing of the thermoset matrix or cooling of thermoplastic matrix in polymer composites, internal stresses appear [24]. These stresses increase the pressure between adjacent particles, giving contact pressure and decreasing the contact resistance. Hence, internal stresses in polymer matrix caused by shrinkage, external mechanical actuation, or thermal expansion play an important role in the conductivity of composites. A shrinkage of polymer during processing can induce high internal stresses. This reduces the interparticle resistance. Instead, the observed strong resistivity change is caused by a release of particle–particle contact pressure and a change in gap distance. Polymer and the conducting filler particles are in a state of close packing with intimate contact to next neighbors, forming conducting paths throughout the composite. During heating, the polymer expands much more than the filler particles themselves. The contact pressure between adjacent filler particles is reduced leading to a moderate resistivity increase.

4.3.6 The Percolation Theory and PTC Effect

According to percolation theory and above PTC theories, the PTC effect of polymer nanocomposites strongly depends on filler content. The PTC curve practically coincides with that of percolation curve (as shown in Fig. 4.1). Conductive particles agglomerate in composite as clusters. As the size and number of clusters increase with increasing filler content, at some critical content, the cluster becomes infinite and makes a contribution to the composite conductivity. The agglomerates of particles in infinite cluster can be abruptly separated, and the composite become dielectric by thermal expansion of polymer matrix. So the greatest PTC effect usually takes place in composites with moderate filler content.

In summary, because these theories cannot be observed by experimental techniques, there has been difficulty in finding a comprehensible explanation for the effect, and thus most of mechanisms still remain controversial.

Although there is no satisfactory theory to explain the PTC and NTC phenomena, all of these models suggest that the volume expansion plays an important role in PTC behavior, and the explanation based on tunneling effect is widely accepted. According to this mechanism, electrons pass through the thin gaps between adjacent CB particles, aggregates, and agglomerates at a practical magnitude of the electrical field. The rapid expansion near the melting point of polymer matrix increases the width of gaps and thus hinders the process of electron tunneling. On the other hand, NTC effect is presumably due to the reaggregation of conductive particles in polymer melting state and therefore reparation of disconnected conductive pathways.

4.4 Influence of Polymer Matrix on PTC Effect of Nanocomposites

The polymer is framework of a nanocomposite, and melting expansion is the main role in PTC effect. Therefore the conductivity of polymer nanocomposites is sensitively influenced by characteristics of polymer matrix such as chemical structure, thermal property, morphology, crystallinity, and processing conditions.

4.4.1 Influence of Polymer Crystallinity on PTC Effect

A number of researchers observed strong correlation between crystallinity and PTC effect. The amorphous polymer PTC composites are hard to obtain great PTC effect because the volume thermal expansion of amorphous polymers is too small to produce significant resistivity change. This has led some scientists to suggest that crystallinity has an influence on electrical conductivity [25–27].

The PTC effect is diminished in nanocomposites of semicrystalline polymers if specimens are quenched rapidly to yield low crystallinity or if crystallinity of specimens is reduced by thermal degradation. On the other hand, increased crystallinity of polymer due to annealing promotes PTC effect. Figure 4.2 shows the resistivity as a function of temperature for various polymer composites loaded with 50 wt % CB [28]. For all the polymer/CB composites, the resistivity increased steadily as the temperature was raised and increased more rapidly near the melting temperature when polymer crystal started to melt. When the temperature of composite approached the melting point of polymer resins, the conduction paths formed of the CB interface were damaged because of the partial melting of polymer crystallites; thus, the resistivity of composites increased drastically. The resistivity reached a

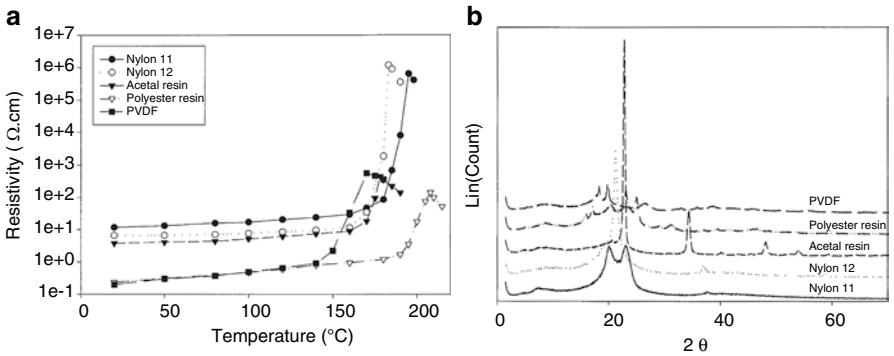

Fig. 4.2 (**a**) Resistivity of various resins/carbon black (50/50 wt %) composites as a function of temperature; (**b**) X-ray diffraction patterns of various polymers (Reprinted with permission from Ref. 28. Copyright 2004 Wiley Periodicals, Inc.)

peak value above the melting temperature and then decreased with a further increase in temperature which is called the NTC effect.

There was a steep increase in resistivity near the melting point of each polymer. The nylon-12 composite had the largest PTC intensity of about 2.0×10^5, although the polyacetal and polyester composites had small PTC intensities. These various PTC intensities were attributed to the difference of crystallinity in the polymer matrix. The larger the crystallinity of the polymer matrix is, the larger the expansion of the polymer becomes when the polymer crystal starts to melt; that is, the conduction path in the composite was effectively interrupted. In these experiments, the crystallinities of the used polymers were measured by X-ray diffractometer at room temperature as shown in Fig. 4.2. As can be seen, the specific crystal peaks of polymer were observed and then were computed. The degrees of crystallinity of the polymer matrices were 48.06 % (nylon-11), 48.30 % (nylon-12), 38.62 % (polyacetal resin), 36.26 % (polyester resin), and 40.91 % (PVDF), respectively. From these data, it was confirmed that the PTC intensity was proportional to crystallinity of polymer.

However, this has been questioned by others. Some experiments do not support a correlation between PTC intensity (the ratio of peak resistivity to the room temperature resistivity) and crystallinity [29–31]. Preparation of an amorphous polymeric PTC composite with PTC intensity of about 10^3 is reported using polyurethane (PU) as matrix and CB as conductive filler and adding reactive low molecular crystals and stearic acid as crystalline phase into polymers [29]. As the stearic acid could melt and expand rapidly in a very narrow temperature range around the melting point, the volume fraction of CB could consequently reduce sharply, which results in the disconnection of conductive channels and cause the amorphous rubbery composite to produce PTC effect. Comparing to crystalline PTC plastics, the amorphous rubbery PTC materials can easily form cross-linking to prevent NTC effect, while it still has rubbery toughness, processability, and moldability. Therefore, it was assumed that the PTC effect is due to the difference of the thermal expansion coefficients between matrix and filler.

4.4.2 Influence of Melting Temperature of Polymer on PTC Critical Temperature

Polymers can show three significant reversible structural transitions, which are thermally induced: crystallization and melting in a semicrystalline phase and a glass transition in the amorphous phase. All three transitions are related to a relative large volume change or to a pronounced change in the thermal expansion.

The improvement on PTC properties of CB-filled semicrystalline polymer composites, such as CB-filled high-density polyethylene (HDPE), poly(vinylidene fluoride) (PVDF), and polypropylene (PP), respectively, has received considerable attention due to its appropriate crystallinity, melting point, processability, and relatively low price [4, 32, 33]. However, one of the great disadvantages that the

semicrystalline used as polymer host is the single temperature at about 130 °C (for HDPE) or 160 °C (for PVDF or PP). From the practical aspect, a difference of the critical temperature at which the PTC anomaly occurs is of special interest in temperature sensor. Recent work in this field has led to a better control of critical temperature.

According to the mechanism mentioned above, the PTC transformation is triggered by the melting of crystalline phase; therefore, the critical transformation temperatures are near the melting points of these polymers and different with the variation of polymer [34, 35]. The PU/CB composite does not have PTC effect in the absence of stearic acid, but it exhibits significant PTC effect and little NTC effect in presence of stearic acid [29]. The critical transformation temperature of PU/CB composites is the melting point of stearic acid (67–71 °C). The critical transformation temperature of polymer-based composites can be adjusted by adding low molecular crystals with different melting points or intermixture immiscible polymer blends to obtain two resistivity jumps which designated as the double-PTC effects. The highest critical transformation temperature was reported above 200 °C [36]. For example, for CB-filled ETFE/HDPE composite, the large thermal expansion owing to the melting of HDPE and ETFE crystallites is responsible for the first and second critical transformation temperature [36]. Akihiko et al. found that the onset of PTC effect with an Ni content of 20 vol.% is approximately 100 °C lower than the melting point of the PVDF matrix [37]. These results are shown in Fig. 4.3.

4.4.3 Influence of Binary-Polymer Blends on Percolation Threshold

It should be strongly stressed that most past investigations on the PTC and NTC effects of CB-filled polymer composites were focused on composites containing CB and a single semicrystalline polymer. However, it is often difficult to reach a suitable conductivity by addition of an amount of CB small enough to preserve the mechanical properties of polymer and to reduce as much as possible the cost of the final composite. Few studies were conducted on the PTC and NTC effects of CB-filled immiscible semicrystalline polymer or multiphase polymeric blends [8, 9, 12–14, 38–41]. The purposes include (1) to obtain a conductive composite with a very low percolation threshold and (2) to provide a new approach to eliminate the NTC effect even at temperatures much higher than the melting point of the polymer.

The selective dispersion of CB in one phase or at the interface of two polymers causes a decrease of the percolation threshold to a very low level. It is proposed that the heterogeneous distribution of CB in immiscible polymer blends is mainly due to the difference in affinity of CB particles to each component of polymer blends, i.e., the difference in the interfacial free energy of the polymer/filler. Gubbels et al. reported the two-step percolation in the LDPE/EVA composite filled with CB [42].

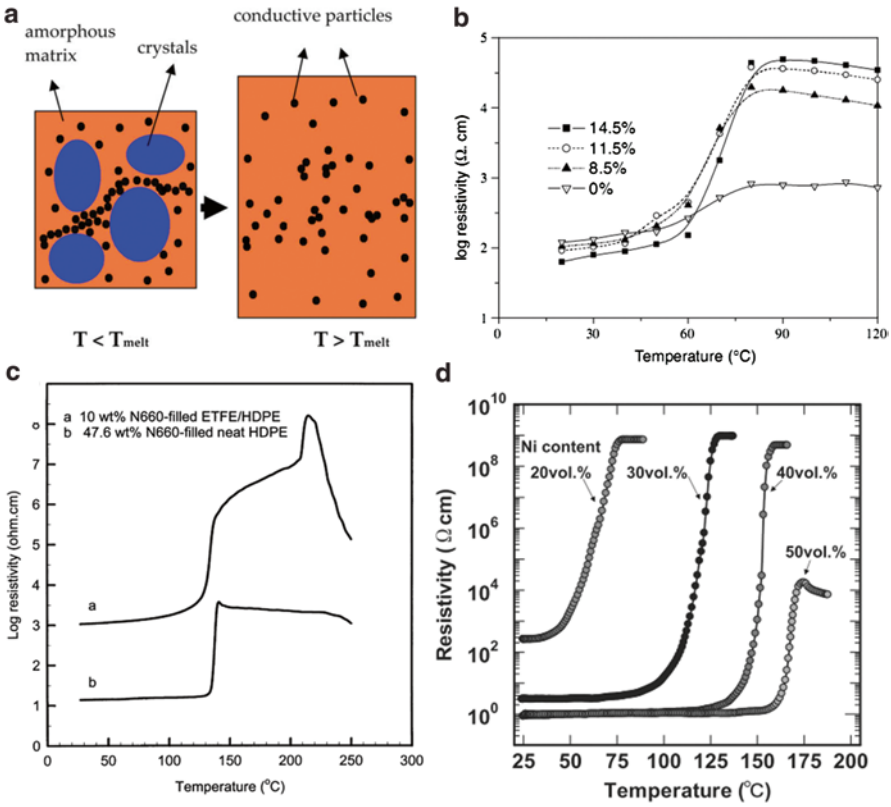

Fig. 4.3 (**a**) Schematic of crystal melting and the origin of the PTC effect in the composites of semicrystalline polymers. Tmelt represents the melting temperature of the crystals. Melting of large amounts of crystals augments the volume and disturbs the connectivity of the conductive particles (Reprinted with permission from Ref. [34]. Copyright 2008 Elsevier Ltd). (**b**) Resistivity of PU/CB composites vs. temperature at different stearic acid content (Reprinted with permission from Ref. [29]. Copyright 2005 Elsevier Ltd). (**c**) Log resistivity of 10 wt% N660-filled ETFE/HDPE(4/1) composite and 47.6 wt% N660-filled neat HDPE composite as a function of temperature (Reprinted with permission from Ref. [36]. Copyright 2000 Elsevier Science Ltd). (**d**) PTC curves of PVDF/Ni composites at Ni content of 20, 30, 40, and 50vol.% (Reprinted with permission from Ref. [37]. Copyright 2012 Elsevier Ltd.)

They thought that CB particles were predominately dispersed in LDPE first due to lower interfacial free energy and then began to be localized at the LDPE/EVA interface when the CB content in LDPE had approached a saturation limit.

Di et al. proposed that the high viscosity of UHMWPE melt will minimize the migration of carbon particles into the polymer matrix and deformation of the polymer particles during the hot compaction [11]. This provides the possibility of reducing the percolation threshold by favoring the heterogeneous distribution of CB particles and eliminating the NTC effect by hindering the movement of CB particles in the UHMWPE melt.

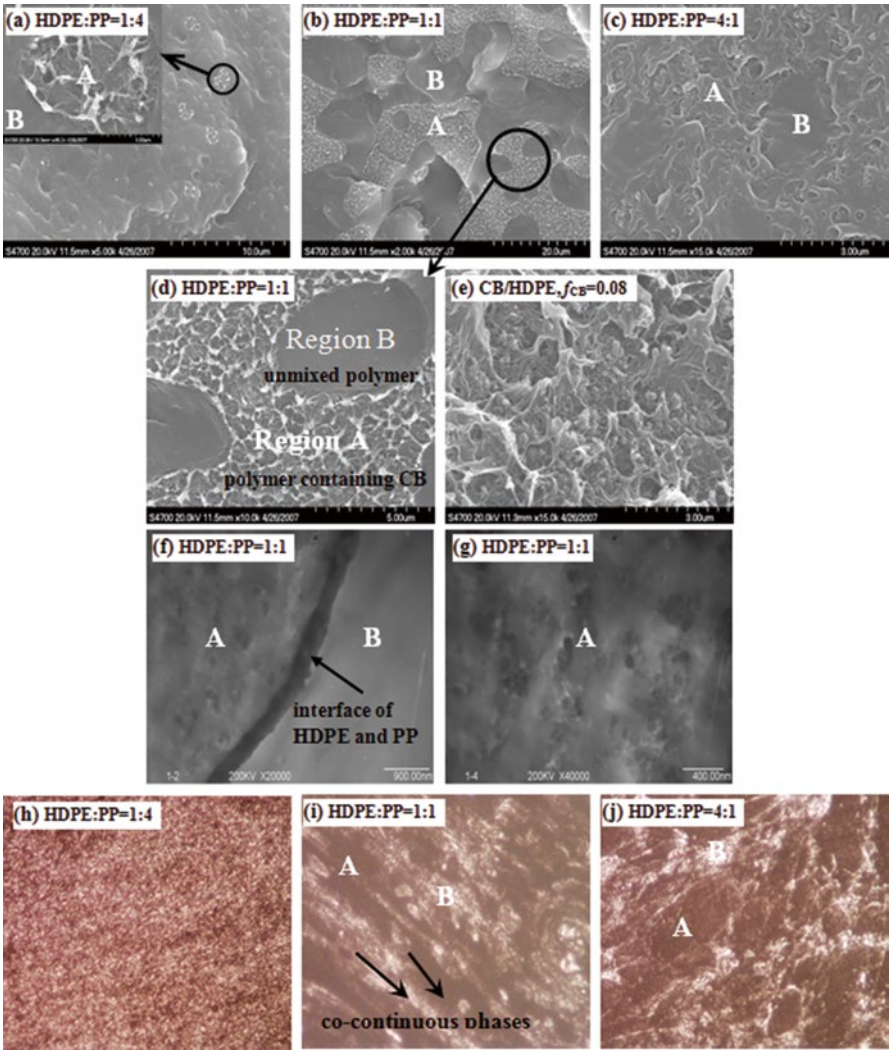

Fig. 4.4 SEM, TEM, and OM images of the (MNCB-HDPE)/PP composites at f_{MNCB} =0.03: (**a**–**c**) SEM images of fracture surfaces of the composites at volume ratios of HDPE:PP =1:4, 1:1, and 4:1; the inset in (**a**) shows a magnified image of the A zone; (**d**) magnified SEM image of the composite at HDPE:PP =1:1; (**e**) SEM image of the fracture surface of the CB/HDPE composite at f_{MNCB} =0.08; (**f**, **g**) TEM images of slices of the composite at the volume ratio of HDPE:PP = 1:1; (**h**–**j**) OM images of the (MNCB-HDPE)/PP thin films at volume ratios of HDPE:PP = 1:4, 1:1, and 4:1, showing that the area of the MNCB-filled HDPE phase (*region A*) increases with increasing volume ratio of HDPE:PP, while the area of the PP phase without MNCB loading (*region B*) decreases (Reprinted with permission from Ref. [39]. Copyright the Royal Society of Chemistry 2008)

Feng et al. have studied the double-PTC effects of CB-filled ETFE/HDPE composites; they observed from the optical microscopy and time-of-flight secondary mass spectrometry results that the CB particles were only selectively localized in the HDPE phase because of the high viscosity of ETFE matrix [13]. Ying et al. also believed that the elimination of the NTC effect and a good reproducibility of LMWPE/UHMWPE blends filled with short carbon fibers were due to the very high viscosity of UHMWPE [11].

Xu et al. present a robust and simple procedure to prepare binary-polymer matrix composites with strong PTC effect [39]. The intuitive and detailed double-percolation structure is observed on basis of morphological evidence as shown in Fig. 4.4. Modified nanoscaled carbon black (MNCB) is often selectively localized in HDPE phase that forms continuous electrically conductive channels in the polymer, and both HDPE and PP phases are also continuous in three-dimensional space. When the volume ratio of the two polymers is very close to 1:1, the remarkable PTC intensity (PTCI), namely, PTCI = 3.3×10^7 in (MNCB-HDPE/PP) nanocomposite, is observed.

4.5 Influence of Conductive Filler on PTC Effect of Nanocomposites

The conventional method of preparing conductive polymer composites is to disperse the conductive fillers such as CB, carbon fiber (CF), graphite, and metal particles, throughout the polymer matrix. The conductivity of polymer composites depends not only on the characteristics of polymer matrix but also on the properties of fillers such as particle size, concentration, dispersion state and aggregate shape, etc. Clarifying the role of all these factors enables us to choose the suitable processing method for obtaining the composites and to improve the electrical characteristics of these systems.

4.5.1 The Kinds of Conductive Filler

The usual conductive fillers used can be classified as carbon system such as CB, CF, graphite, and metallic system such as nickel (Ni), copper (Cu), and zinc (Zn). The superconductive materials can act as a potential filler to be used in PTC materials.

4.5.1.1 Carbon System Filler

The use of polymer conductive composites based on carbon fillers (like carbon black, carbon nanotube, graphite, graphene, carbon fiber, metal-coated carbon fiber, etc.) was found to be superior in many electrical and electronic applications

compared to metals because of their lightweight, low cost, and oxidation resistance. An increasingly important use for CB is as the filler in polymers in order to enhance the electrical conductivity of the polymer. CB varies greatly in their structure. The structural characterization of these materials is difficult because of the very small particle size in the materials. In general, the structures are described as being either a high structure or a low structure. A high-structure CB usually consists of many primary particles of CB fused together in an aciniform aggregate structure. A low-structure CB consists of a small number of CB particles fused together in an aggregate, generally with a larger primary particle size. The use of CB of different structures will affect the conductivity in a given polymer system to varying extents. Normally a polymer loaded with a high-structure CB or a CB with a small particle size will have a lower electrical resistivity than a CB which possesses a low structure or large particle size, at the same CB concentration in a composite [43, 44].

Natural graphite is a well-known material with good electrical conductivity and has been extensively applied to make polymer/graphite composites [45]. The use of expanded graphite in polymer/graphite composites will greatly enhance their electrical conductivity. In addition, it is interesting to note that graphite has different conductivities at different directions.

The electrical conductivity of CF is between CB and graphite. The high aspect ratio of CF would affect the physical and mechanical properties of the synthesizing polymer composites. But the higher cost limits the usage of CF. It can be considered as the second conductive filler, which are considerably longer than the CB particles to bridge distant and unconnected CB particles and which are more likely to form conductive pathways within the polymer blend [46–49].

The PTC effect of electrical resistivity of UHMWPE/LDPE/CF nanocomposites was investigated by Zhang et al. as shown in Fig. 4.5. Figure 4.5a reveals a typical percolation curve of resistivity, and the scaling law demonstrated by Ref. [50] gives f_c of 2.4 vol.%. Comparing with the CB/UHMWPE composites, f_c of UHMWPE/LDPE/CF composites was much lower. The low f_c is mainly attributed to the large aspect ratio of CF and is also influenced by the binary phase of different matrices. From Fig. 4.5b, we can see all specimens exhibited obvious PTC effect. The PTC effect occurred at different temperatures for different samples which increase with CF content evidently, not at a constant temperature. The PTC intensity was enhanced firstly and then decreased with increasing CF content.

The CNTs have been used extensively as conductive filler in different polymer matrices and reported to increase the electrical conductivity of the composites at relatively low concentration [51–55]. Gao et al. reported that the PTC intensity of the CNT/HDPE composites is lower than that of CB/HDPE composites, which is due to the entanglement between CNTs [56]. It is found from Fig. 4.6 that the CNT/HDPE thermistors exhibit much larger hold current and higher hold voltage than the commercial CB/HDPE thermistors; such high voltage-bearing or current-bearing capacity for the CNT/HDPE thermistors is mainly attributed to the high thermal conductivity and heat dissipation of entangled CNT networks. Moreover, the CNT/HDPE also exhibits quick response of current decay to applied voltages, comparable to the commercial CB/HDPE thermistors [57].

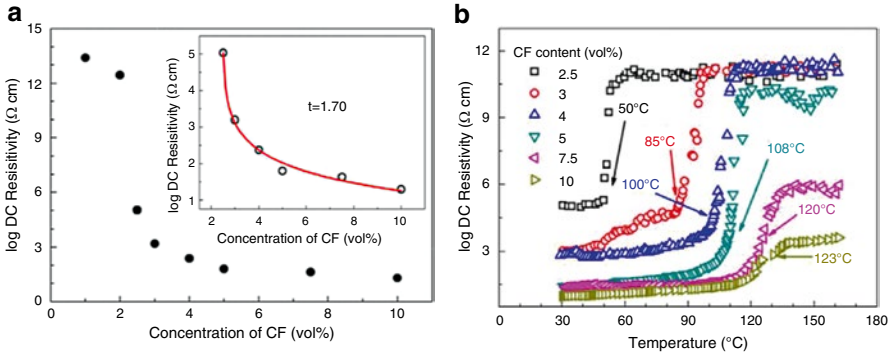

Fig. 4.5 (**a**) DC resistivity of UHMWPE/LDPE/CF composites against CF concentration at room temperature, the inset is the calculation and experimental results (*black open circles*) according to the scaling law; (**b**) PTC effect of UHMWPE/LDPE/CF with CF contents of 2.5–10 vol.% (Reprinted with permission from Ref. [50]. Copyright 2014 Elsevier Ltd.)

Graphene has a large aspect ratio, exceptionally high mechanical strength and superior electrical and thermal conductivity. Thus, it can replace CNTs for reinforcing polymers to form electrically conductive polymer nanocomposites. It has been reported that graphene-based polymer nanocomposites exhibit better electrical and mechanical properties than the CNT/polymer composites [58–60].

In Fig. 4.7, Seung et al. incorporated a novel type of electrochemically exfoliated graphene sheets (EGs) fillers into poly(methyl methacrylate) (PMMA) polymer matrices. Without the conventional oxidation/reduction process to prepare the graphene-based fillers, the EGs/PMMA polymer nanocomposites showed the high electrical conductivity of $417 \pm 83 Sm^{-1}$ at a content loading of 5.8 vol.% and a low percolation threshold of 0.37 vol.% [60].

4.5.1.2 Metal or Metal Ceramic System Filler

Polymer nanocomposites filled with conductive metal particles are of interest for many fields of engineering [61–64]. The interest arises from the fact that the electrical characteristics of such nanocomposites are close to the properties of metals, whereas the mechanical properties and processing methods are typical for plastics. It was observed experimentally that the electrical conductivity and the PTC effect of metal–polymer nanocomposite predominantly depend on the electrical conductivity, the particle shape and size, and the volume fraction and the spatial arrangement of the metal particles. In the present studies, aluminum, nickel, iron, zinc, and copper powders with essentially different particle shapes (irregular, dendritic, and almost spherical) as well as the metal ceramic compounds such as TiB_2, TiC, NbB_2, WSi_2, $MoSi_2$, V_2O_3, and VO_2 were used as conductive fillers. However, the usage of metallic fillers in PTC composites is limited to some extent because of the easy

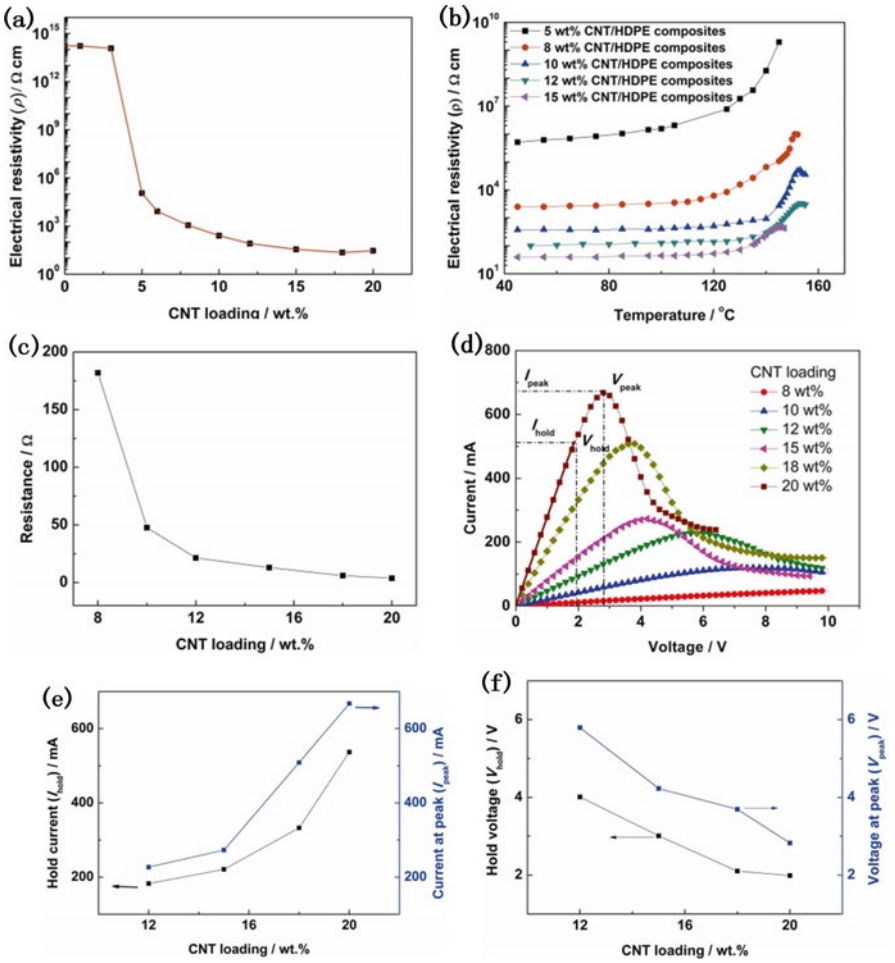

Fig. 4.6 Electrical properties of the CNT/HDPE composites. Electrical resistivity (r) of the CNT/HDPE composites as a function of (**a**) CNT loadings and (**b**) temperature; (**c**) electrical resistance of the CNT/HDPE thermistors at room temperature; (**d**) voltage–current curves of the CNT/HDPE thermistors, implying a typical PTC effect induced by applied voltages; (**e**) hold current and (**f**) hold voltage of the thermistors as functions of CNT loadings (Reprinted with permission from Ref. [57])

oxidation of the surface, and the surface oxide layers formed may decrease the conductivity. Moreover, the high cost of the metallic fillers is another reason for limiting the widely application.

Andrzej et al. studied the nanocomposites based on polymer blends of HDPE and polybutylene terephthalate (PBT), filled with dispersed silver nanoparticles (Ag) [65]. It was found from Fig. 4.8 that depending on the choice of CPC structure,

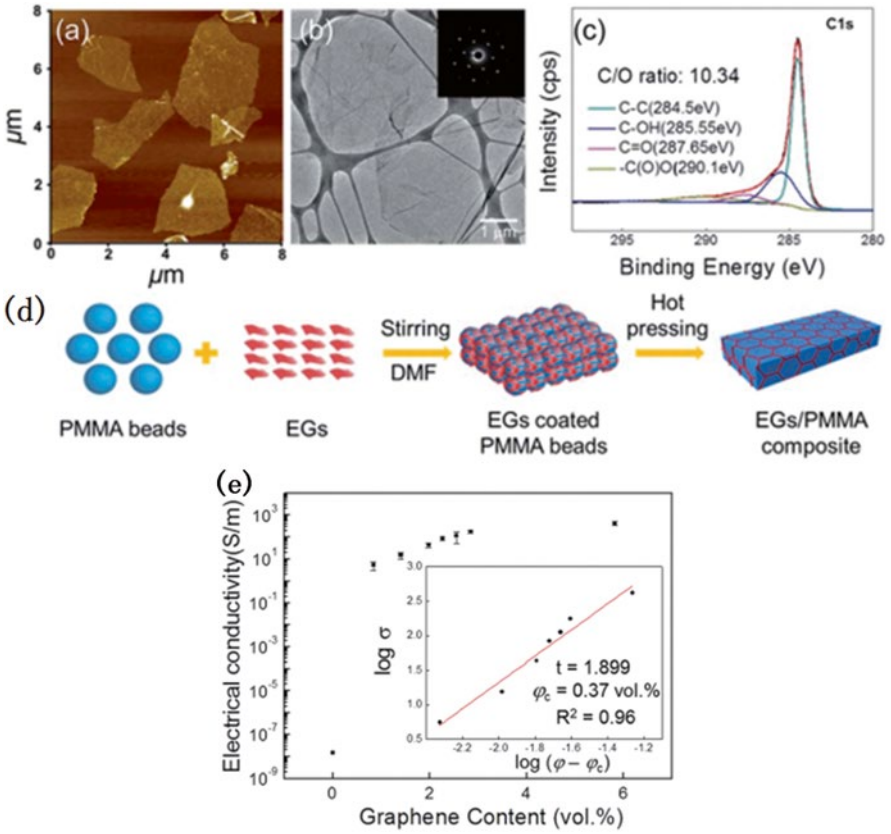

Fig. 4.7 Morphology, thickness, and chemical structure of EGs characterized using (**a**) AFM, (**b**) TEM, and (**c**) XPS; (**d**) schematic illustration of EGs/PMMA composites with the segregated networks of EG fillers. (**e**) Semi-log plot of electrical conductivity of the EGs/PMMA composites as a function of EG filler content (Reprinted with permission from Ref. [60]. Copyright the Royal Society of Chemistry 2015)

the commutation temperature from a conducting state to an insulating state can be observed between 45 and 180 °C. The observed high intensity of PTC effect, i.e., a sharp (narrow temperature range) and strong (10 orders of magnitude) resistivity increase, makes such composites promising for current limiting devices and temperature sensors.

Mitsuhiro et al. have focused on titanium carbide (TiC) from particles with conductivity and thermal conductivity superior to CB as conductive particles to be used in a high-polymer PTC thermistor [66]. Figure 4.9 shows the PTC characteristics of TiC/PE composites. The resistivity showed positive temperature dependence and changed abruptly in the tenth order of its magnitude during the melting transition of PE. The electrical current cutoff characteristics of the samples indicated excellent

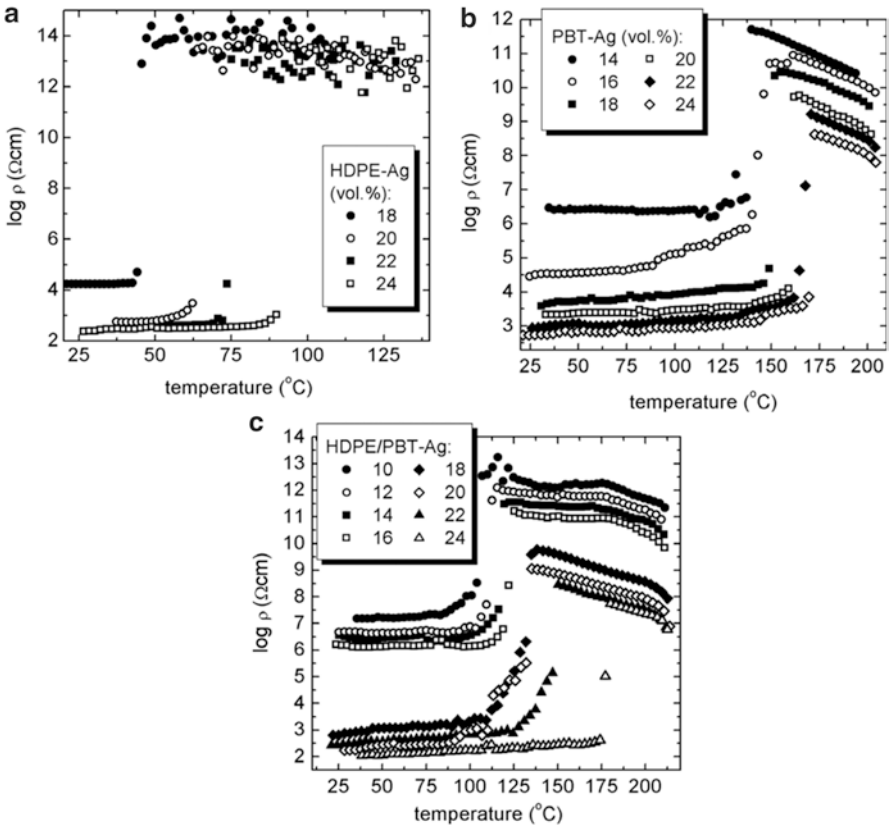

Fig. 4.8 (**a**) The values of the resistivity vs. temperature for HDPE–Ag composites with different contents of the filler; (**b**) temperature dependence of the resistivity of PBT–Ag composites filled with the different volume fractions of Ag; (**c**) temperature dependence of resistivity for the HDPE/PBT–Ag composites with different volume fractions of Ag (Reprinted with permission from Ref. [65]. Copyright 2009 Elsevier Ltd.)

features in the overcurrent response despite their low resistivity values, as compared with those of other PTC materials.

4.5.1.3 Morphological Control Through a Mixed Filler

To achieve a lower percolation threshold or a lower cost, more than one type of fillers, particularly fillers with different aspect ratios, can be used to prepare PTC nanocomposites [33, 67–71]. These hybrid fillers, which contain different carbon fillers, such as CNTs, CF, graphite-based fillers, and CB, are often used due to their distinctly different aspect ratios and similar carbon-based structures.

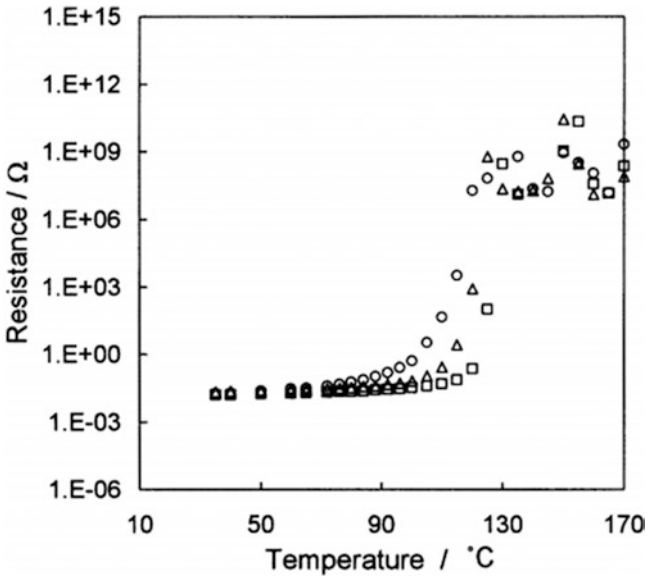

Fig. 4.9 T–R characteristics of TiC/PE composites. f=0.54 (O); 0.58 (Δ); 0.62 (γ) (Reprinted with permission from Ref. [66]. Copyright 2005 Wiley Periodicals, Inc.)

As shown in Fig. 4.10, the percolation thresholds of these systems are often near or below the average of the systems that are filled with a particular type of carbon filler, indicating that a considerable amount of a high aspect ratio and high price filler can be replaced with a low aspect ratio and low price filler [72]. It has been reported that a low aspect ratio filler can act as a bridge between the networks that are formed by the high aspect ratio filler [71] or form special configuration conductive networks with the high aspect ratio filler [33].

In Fig. 4.11, by introducing 0.5 vol.% CNTs into the 4 vol.% CB-filled UHMWPE0.8–PVDF0.2 composites, the initial resistivity decreased by about two orders of magnitude, and the PTC intensity increased by about 30 %. Owing to the three-dimensional conductive networks provided by tube-shaped CNTs and spherical CB and the high viscosity of the UHMWPE matrix, favorable PTC repeatability was also achieved [73].

4.5.2 The Grain Size and Morphology of Conductive Filler

Polymer materials in their pure state are excellent electrical insulators, which can also become conductors when filled with various kinds of conductive particles. In general, the electrical conduction process in conductive polymer composites is

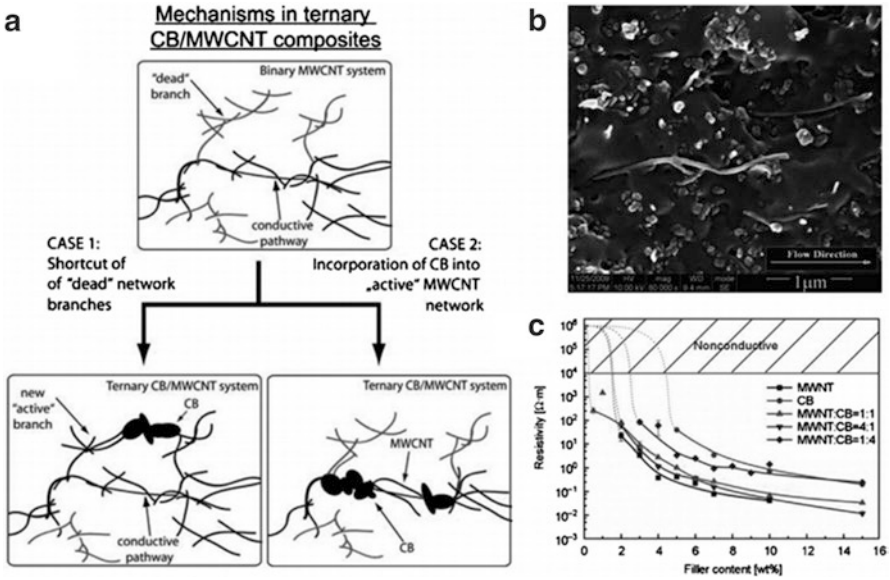

Fig. 4.10 (**a**) The mechanism of synergistic effect between MWNT and CB for the formation of conductive network in CPCs based on epoxy matrix (Reprinted with permission from Ref. [71]. Copyright 2009 Springer Science Business Media); (**b**) the grape cluster-like conductive network constructed by CB and oriented MWNTs in PP matrix (Reprinted with permission from Ref. [33]. Copyright 2012 Elsevier Science Ltd); (**c**) the electrical percolation behavior of CPCs based on PP containing different fillers or hybrid fillers, showing lower percolation threshold can be obtained for CPCs containing MWNT and CB in the ratio of 1:1 (Reprinted with permission from Ref. [68]. Copyright 2012 BME-PT)

complicated and dependent on a large number of parameters, mainly on filler concentration. In addition to the amount of loading, filler particle size and morphology structure, filler–matrix interactions, and processing techniques are key factors in determining the physical properties [74, 75].

4.5.2.1 Effect of Filler Size

Experimental data supported that the composite loaded with the larger average filler size exhibits a higher PTC intensity and room temperature resistivity than those composites with the same filler content. The reason for this difference in the PTC intensity lies on the fact that the entanglement between the particles and polymer chains increases and the number of conductive pathways is smaller and the resistivity of the composite is sensitive to even a small decrease in the number of conductive paths. For example, the degree of entanglement between a large-sized CB and the polymer chains is much higher than that between a small-sized CB and the

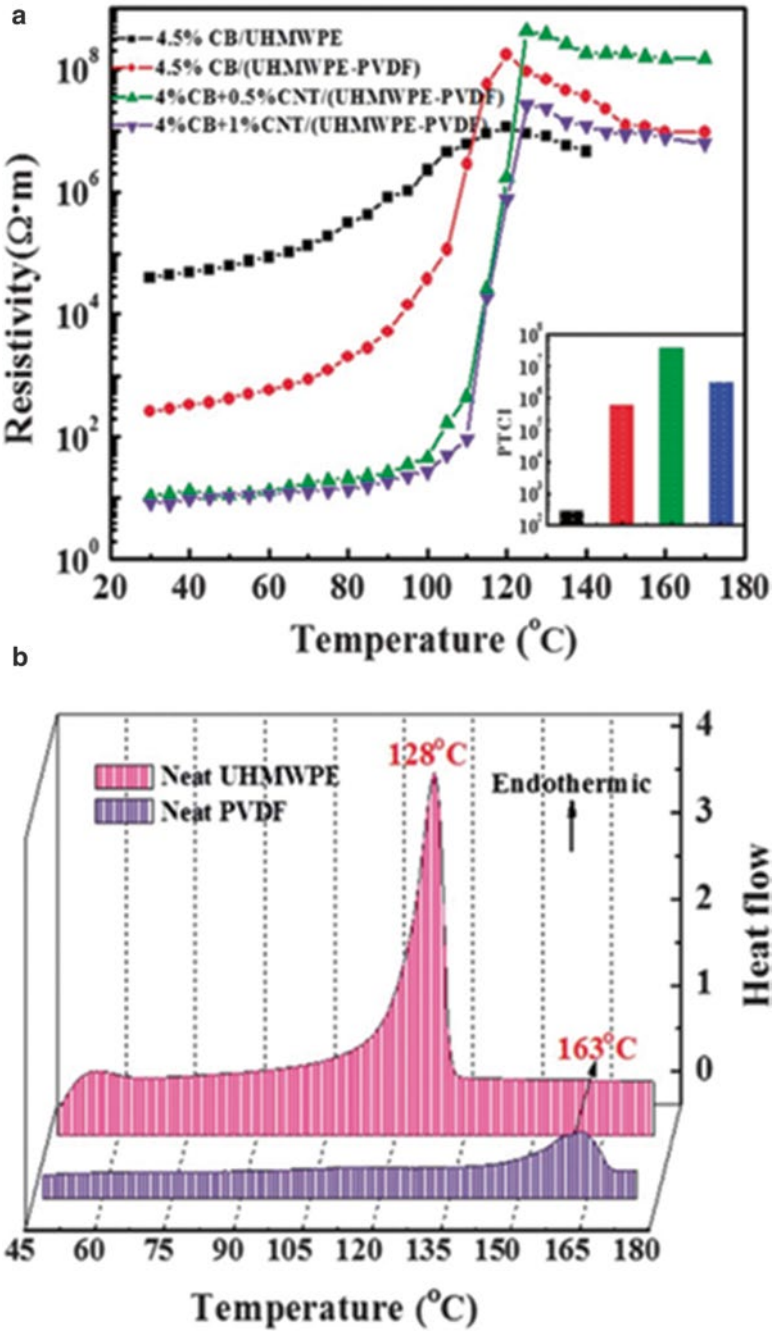

Fig. 4.11 (**a**) Resistivity of the single UHMWPE and UHMWPE0.8–PVDF0.2 based composites with different volume fractions of CB and CNTs as a function of temperature. The inset is their PTC intensities and the same color represents the same system. (**b**) DSC thermograms of neat PVDF and neat UHMWPE (Reprinted with permission from Ref. [73]. Copyright the Royal Society of Chemistry 2013)

polymer chains; thus, the movement of the polymer chains caused by thermal expansion due to the melting of the crystallites may introduce a major deformation of the conductive network structure and break up a large number of the conductive paths. Therefore, composites with a larger particle-size CB show a higher PTC intensity, but their room temperature resistivity is usually higher. This is a major disadvantage for the use of large CB particles in many industrial applications. A balance between the PTC intensity and the room temperature resistivity is then attempted by using a mixture of large-sized and small-sized CB particles in the composites.

4.5.2.2 Effect of Filler Shape

In the previous sections, spherical particles were always assumed in modeling the composites. In practice, however, fillers are often used which have a shape very much different from a sphere. Examples are aluminum flakes, stainless steel fibers, or carbon fibers. The percolation threshold can be drastically reduced for particles with an aspect ratio larger than one. One can easily apperceive that fibers with high aspect ratio can drastically increase the connecting paths and reduce the percolation threshold. Carbon fibers with an aspect ratio of 1000 need only 1.0 vol.%, whereas fibers with an aspect ratio of 10 need a volume fraction of about 10 % in order to achieve the same resistivity [76].

4.5.2.3 Effect of Filler Distribution

The conductive properties depend strongly on the distribution of filler particles in a composite, and the distribution state of filler particles is mainly influenced by the chosen processing technique. For industrial production, extrusion or injection molding processes are used quite often. Using fibers, flakes, or carbon black, the high shear forces occurring at the nozzle, both methods cause an alignment of the filler particles in the flow direction. Hence, the orientation of the fibers or flakes in the final part depends strongly on the form of the mold and the flow of the polymer.

Care must be taken if composite parts are made by compression molding of polymeric and conductive powders. The carbon black particles are much smaller than the polymer particles. This results in a core–shell structure. The polymer particles are surrounded by shells of carbon black, forming a percolating network. The percolation threshold of a core–shell structure is considerably lower than that of homogeneous composite. A controlled orientation of filler particles and an anisotropic conductivity can be achieved by applying electrical or magnetic fields during the processing. This can serve not only for relative high conductivity at low filler content but also for unidirectional conductivity.

4.6 The Effective Ways to Improve the PTC Properties of Nanocomposites

Research and development activities on PTC materials have brought successful industrial applications, and an enormous amount of knowledge has been accumulated in this field. Nevertheless, many problems are not solved yet. Polymer PTC composites have some shortcomings, such as unstable electrical reproducibility due to irregular structure changes in heating/cooling cycles, NTC phenomena, and the slow response rate of PTC effect associated with an adverse effect on desired switching properties. Several ways which include cross-linking, filler treatment, and polymer blends are introduced to increase stability of PTC materials.

4.6.1 Surface Modification of Conductive Filler

The conductive filler, especially for CB, produces large cohesive strength between the individual fine particles, which leads to aggregates of particles, having diameters of not less than several microns. Therefore, it is extremely difficult for CB to be dispersed on the order of submicrons in the medium. So it is very necessary to make a suitable modification on the CB surface in order that it can be more evenly dispersed in the matrix and the interfacial interaction between CB and polymer can be strengthened. Relevant developments in polymer blends based on CB with surface modification such as grafting cross-linking, plasma sputtering, gasification etching, and emulsion polymerization have shown very efficient in improving dispersion behavior and morphological stabilization [77–79], yet the common dispersants would only have a reaction with surface of fillers and not with the molecule of polymers. Grafting a coupling agent to the CB surface can be considered as one of the options to deal with these problems. The coupling agent such as titanate coupling agent (NDZ-102) or silane coupling agent (KH550) has two quite different chemistry reactive groups in the molecule structure, which can react with inorganic filler forming the firm chemical bonds and synchronously link with the organic polymer molecules through physical entanglement or chemical cross-linking, respectively, bridging the filler and polymer tightly together [78]. That is, the filler can be soaked better in the polymer to improve the compatibility of the composite (Fig. 4.12).

He et al. reported a nanocomposite with nanosilver-decorated reduced graphene oxide (Ag–RGO) sheets incorporated into PVDF resulting in a low percolation threshold of 0.17 vol.% [80]. The synthesized Ag–RGO hybrid sheets were proved to be more effective in improving the electrical conductivity of polymer composites when compared to RGO sheets. This was attributed to high intrinsic electrical conductivity of silver. Figure 4.13 illustrated the step procedures of preparing stable Ag–RGO suspension and the PTC effect, making it attractive for a variety of smart device applications.

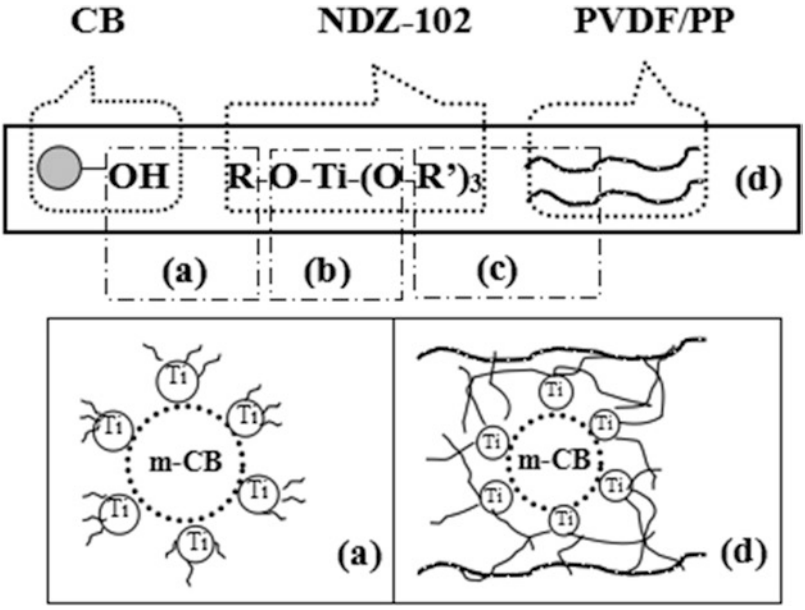

Fig. 4.12 Schematic image of chemical reaction mechanism of NDZ-102 on the interface of CB and polymer (**a**) chemical bond of R groups in NDZ-102 with hydroxyls in CB to form a single molecule layer of coupling agent on CB surface, (**b**) cross-linking action of NDZ-102 with CB and PVDF/PP through conversion reaction of lactones groups, (**c**) physical entanglement and chemical cross-linking of R' with polymer molecules, and (**d**) the enhanced interface between CB and polymer

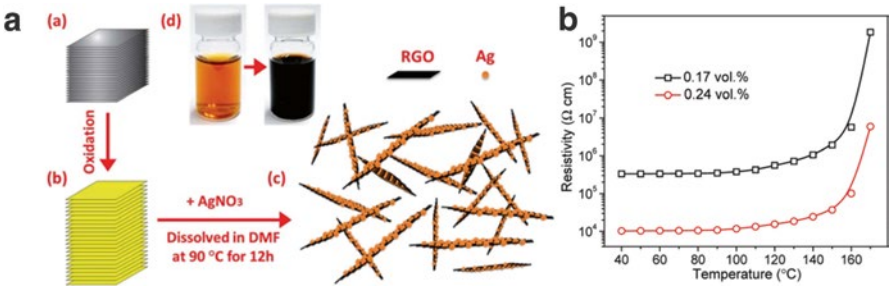

Fig. 4.13 (**a**) Route for synthesizing Ag–RGO hybrid sheets. (*a*) Graphite flake, (*b*) graphite oxide, (*c*) Ag–RGO sheets obtained by dissolving graphite oxide and AgNO3 in DMF and keeping the solution at 90 °C for 12 h, and (*d*) DMF reduction of Ag + and GO to Ag–RGO, changing brown color of the suspension to black; (**b**) effect of temperature on resistivity of Ag–RGO/PVDF composites with 0.17 vol.% and 0.24 vol.% filler loadings (Reprinted with permission from Ref. [80]. Copyright the Royal Society of Chemistry 2015)

4.6.2 The Cross-Linked Polymer Nanocomposites

Researchers have proposed and developed many methods to eliminate the NTC effect of nanocomposites. Among these methods, the first approach used is to cross-link the semicrystalline polymer matrix by a cross-linking agent [81–84]. For instance, Narkis et al. successfully used a peroxide to cross-link CB-filled HDPE composites without sacrificing the PTC intensity [85, 86]. In addition to the use of a cross-linking agent, gamma and electron-beam radiations have been used to cross-link polymer composites [87, 88]. It was mentioned that a third filler could be used to stabilize the polymer matrix and eliminate the NTC effect. The absence of the NTC effect in the cross-linked polymer composites is related to an increase in the viscosity of the polymer matrix, leading to a significant reduction in the mobility of the CB particles in the composites. Based on this idea, it is possible to use a very high viscosity semicrystalline polymer matrix to eliminate the NTC effect.

The effect of electron-beam (EB) irradiation on the PTC/NTC behaviors and the electrical reproducibility of CB/HDPE nanocomposites for PTC switch were investigated by Seo et al. in terms of EB irradiation intensity in a dosage of 30–150 kGy [89]. The NTC behavior was disappeared from a dosage of 60 kGy. It was also found that the EB irradiation led to an improvement of electrical reproducibility of the composites, which was probably due to the reduction of free movement of CB particles at above the melting temperature of HDPE polymer crystalline regions, resulting from increasing the cross-linking structure of CB/HDPE composites. The schematic diagram of electron-beam apparatus for cross-linking, PTC intensity, and electrical reproducibility of polymer nanocomposites is shown in Fig. 4.14.

4.6.3 Heat Treatment of the Nanocomposite

Heat treatment and annealing can improve the crystallization of polymers and enable the fillers to arrange more regularly, so they are good means of improving PTC characteristics of a polymer composite [90, 91]. Cheng et al. prepared a new kind of shape-stabilized phase change materials (PCMs) with PTC effect by adding graphite powder (GP) to the paraffin/LDPE composite (Fig. 4.15) [25]. The heat treatment was done by keeping the temperature of the samples at 70 °C for 5 min. They found that after the process of heat treatment, the NTC effect of the PCMs was eliminated effectively. In addition, the microstructure of the material became more uniform than that without the heat treatment, and the PTC curves were much more stable as a result.

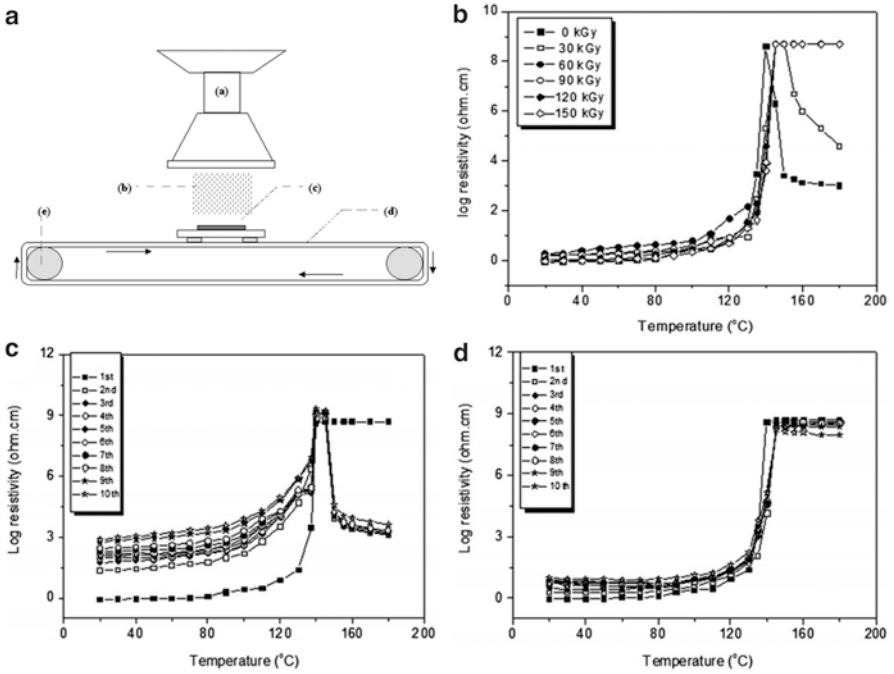

Fig. 4.14 (**a**) Schematic diagram of apparatus for cross-linking of polymer: (*a*) electron-beam accelerator, (*b*) electron beam, (*c*) irradiating sample, (*d*) conveyer, and (*e*) motor; (**b**) PTC intensity of CBs/HDPE conducting polymer composites as a function of irradiation dose; (**c**) electrical reproducibility of unirradiation CBs/HDPE composites; (**d**) electrical reproducibility of CBs/HDPE composites with 60 kGy irradiation dose (Reprinted with permission from Ref. [89]. Copyright 2010 Elsevier B.V.)

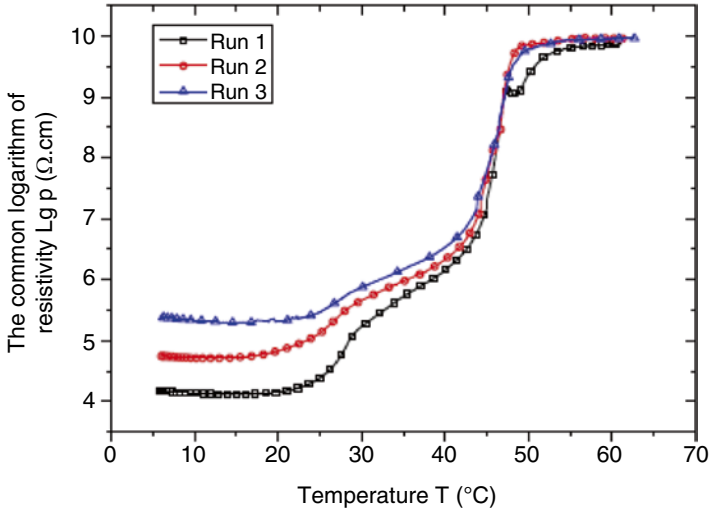

Fig. 4.15 The three runs of the PTC curve for the same sample with the mass fraction (%) of GP/LDPE/Paraffin is 40/18/42. Run 1 was the R–T curve of the sample without heat treatment; Run 2 and Run 3 were the R–T curves of the same sample with heat treatment, which indicated that the NTC effect had disappeared after the heat treatment. In addition, the curve trends of Run 2 and Run 3 in each figure were very similar and much more stable than that of Run 1 (Reprinted with permission from Ref. [25]. Copyright 2014 Published by Elsevier Ltd.)

4.7 Conclusions

In conclusion, research and development activities on PTC nanocomposites have brought successful industrial applications as temperature sensors, self-regulated heaters, and overcurrent protectors. An enormous amount of knowledge has been accumulated in this field. It is assumed that the PTC effect is due to the difference of the thermal expansion coefficients between matrix and filler, and melting expansion of semicrystalline polymer is the main role in PTC effect. Therefore the PTC properties of polymer nanocomposites are sensitively influenced by characteristics of polymer matrix such as thermal property, morphology, crystallinity, and processing conditions. In terms of temperature sensing, the transition temperature can be determined by the melting temperature, the glass transition temperature of the polymer matrix.

Recently, few studies are conducted on the PTC effects of conductive filler-filled immiscible semicrystalline polymer or multiphase polymeric blends. The selective dispersion of fillers in one phase or at the interface of two polymers causes a decrease of the percolation threshold to a very low level, which contributes to being processed with ease, preserving the mechanical properties of the polymer and reducing as much as possible the cost of the final composite. It is proposed that the heterogeneous distribution of fillers in immiscible polymer blends is mainly due to the difference in affinity of fillers to each component of polymer blends, i.e., the difference in the interfacial free energy of the polymer/filler.

The use of PTC nanocomposites based on carbon fillers, such as CB, CNTs, CF, graphite, graphene, metal-coated carbon fiber, etc. is found to be superior in many applications compared to metals because of their lightweight, low cost, and oxidation resistance. In addition to the amount of loading, filler particle size and morphology structure, filler–matrix interactions, and processing techniques are also key factors in determining the PTC properties.

Many efforts to achieve morphological control over the conductive networks in nanocomposites have attracted significant attention due to the vital role that morphology plays in PTC properties. To achieve a lower percolation threshold or a lower cost, more than one type of filler, particularly fillers with different aspect ratios, can be used to prepare PTC nanocomposites. These hybrid fillers, which contain different carbon fillers, such as CNTs, CF, graphite-based fillers, and CB, are often used due to their distinctly different aspect ratios and similar carbon-based structures.

Nevertheless, many problems are not solved yet. Polymer PTC nanocomposites have some shortcomings, such as unstable electrical reproducibility due to irregular structure changes in heating/cooling cycles, NTC phenomena, and the slow response rate of PTC effect associated with an adverse effect on desired switching properties. Recently the extensive progress on several efficient methods for controlling the morphology of conductive networks to increase stability of PTC materials has been developed, which include cross-linking the semicrystalline polymer matrix by a cross-linking agent, gamma and electron-beam radiations, grafting functional chemical groups or polymer molecules onto the surface of the conductive fillers,

etc. It is believed that the elimination of the NTC effect in the cross-linked polymer composites is related to an increase in the viscosity of the polymer matrix, leading to a significant reduction in the mobility of the fillers in the composites. Based on this idea, it is possible to use a very high viscosity semicrystalline polymer matrix to eliminate the NTC effect. Heat treatment and annealing can improve the crystallization of polymers and enable the fillers to arrange more regularity, so they are good means of improving PTC characteristics of a polymer nanocomposite.

References

1. Király A, Ronkay (2015) Polym Test 43:154–162
2. Tan Y, Song Y, Cao Q, Zheng Q (2011) Polym Int 60:823–832
3. Lu C, Hu XN, He YX, Huang X, Liu JC, Zhang YQ (2012) Polym Bull 68:2071–2087
4. Ram R, Rahaman M, Khastgir D (2015) Compos: Part A 69:30–39
5. Brigandi PJ, Cogen JM, Wolf CA, Reffner JR, Pearson RA (2015) Kinetic and thermodynamic control in conductive PP/PMMA/EAA carbon black composites. J Appl Polym Sci 25:132–137
6. Feng C, Jiang L (2013) Compos Part A: Appl Sci Manuf 47:143–149
7. Cheng WL, Zhang RM, Xie K, Liu N, Wang J (2010) Sol Ener Mat Sol Cells 94:1636–1642
8. Frydman E (1945) UK Patent Spec. 604 195 I718 14S, 1945
9. Cheng WL, Song JL, Wu WF (2012) Spacer Eng 21:131–135
10. Kar P, Khatua BB (2011) Polym Eng Sci 51:1780–1790
11. Ying X, Hisako I, Zhen BY (2004) M Masaru Carbon 42:1699–1706
12. Di WH, Zhang G, Peng Y, Zhao ZD (2004) J Mater Sci 39:695–697
13. Chen R, Bin YZ, Zhang R, Dong EY, Ougizawa T, Kuboyama K, Mastuo M (2012) Polymer 53:5197–5207
14. Srivastava S, Tchoudakov R, Narkis M (2000) Polym Eng Sci 40(7):1522–1528
15. Struèmpler R. Glatz-reichenbach J (1999) J Electroceram 3:4, 329–346
16. Sumita M, Sakata K, Asai S, Miyasaka K, Nakagawa H (1991) Polym Bull 25:265–271
17. Nakamura S, Saito K, Sawa G, Kitagawa K (1997) Jpn J Appl Phys 36:5163–5168
18. Kohler F (1966) Resistance element. US Patent, 3,243,753, 1966
19. Ohe K, Natio Y (1971) Jpn J Appl Phys 10:199–208
20. Meyer J (1973) Polym Eng Sci 13:462–486
21. Klason C, Kubat J (1975) J Appl Polym Sci 19:831–845
22. Voet A (1980) Rubber Chem Tech 54:42–50
23. Allak HK, Brinkman AW (1993) J Mater Sci 28:117–120
24. Mamunya YP, Zois H, Apekis L (2004) Powder Tech 140:49–55
25. Cheng WL, Wu WF, Song JL, Liu Y, Yuan S, Liu N (2014) Ener Conversion Manag 79:470–476
26. Brigandi PJ, Cogen JM, Wolf CA, Reffner JR, Pearson RA (2015) J Appl Polym Sci 132:42134
27. Dai K, Zhang YC, Tang JH, Ji X, Li ZM (2012) J Appl Polym Sci 125:561–570
28. Kim J, Kang PH, Nho YC (2004) J Appl Polym Sci 92:394–401
29. Xiong CX, Zhou ZY, Xu W, Hu HR, Zhang Y, Dong LJ (2005) Carbon 43:1778–1814
30. Jiang MJ, Dang ZM, Xu HP (2007) Appl Phys Lett 90:042914
31. Wan Y, Xiong CX, Yu JY, Wen DJ (2005) Comp Sci Tech 65:1769–1779
32. Kar P, Khatua B (2010) J Appl Polym Sci 118:950–959
33. Wen M, Sun X, Su L, Shen J, Li J, Guo S (2012) Polymer 53:1602–1610
34. Gunes IS, Jimenez1 GA, Jana SC (2009) Carbon 47:981–997
35. Ibarrola JMA, Lopez SH, Santiago EV, Pe´rez JA, Valverde MIP (2015) J Thermoplast Compos Mater 28(4):574–590

36. Feng JY, Chan CM (2000) Polymer 41:7279–7282
37. Akihiko K, Katsuya S, Hajime N, Yousuke G, Yusuke K, Toshiaki O, Hideo H (2012) Polymer 53:1760–1764
38. Xu HP, Dang ZM, Yao SH, Jiang MJ, Wang DY (2007) Appl Phys Lett 90:152912
39. Xu HP, Dang ZM, Shi CY, Lei QQ, Bai J (2008) J Mater Chem 18(23):2685–2690
40. Zhang SM, Deng H, Zhang Q, Fu Q (2014) Appl Mater Interfaces 6:6835–6844
41. Dai K, Qu YY, Li Y, Zheng GQ, Liu CT, Chen JB (2014) Tuning of the PTC and NTC effects of conductive CB/PA6/HDPE composite utilizing an electrically superfine electrospun network. Mater lett 114:96–99
42. Gubbels F, Jerome R, Vanlathem E, Deltour R, Blacher S, Brouers F (1998) Chem Mater 10:1227–1235
43. Nicolaus P, Eusebiu G (2002) Carbon 40:201–205
44. Mather PJ, Thomas KM (1997) J Mate Sci 32:401–407
45. Wang WP, Pan CY, Wu JS, Phys J (2005) Chem Solid 66:1695–1700
46. Lee JH, Kim SK, Kim NH (2006) Scripta Mater 55:1119–1122
47. Feller JF, Linossier I, Grohens Y (2002) Mater Lett 57(1):64–71
48. Das NC, Chaki TK, Khastgir D (2001) Adv Polym Tech 20:226–236
49. Zhang YC, Dai K, Pang H, Luo QJ, Li ZM, Zhang WQ (2012) J Appl Polym Sci 124:1808–1814
50. Zhang R, Tang P, Li JF, Xu DG, Bin YZ (2014) Polymer 55:2103–2112
51. Ke K, Wang Y, Luo Y, Yang W, Xie BH, Yang MB (2012) Compos Part B 43:3281–3287
52. Jiang SL, Yu Y, Xie JJ, Wang LP, Zeng YK, Fu M, Li T (2010) J Appl Polym Sci 116:838–842
53. Chen J, Shi YY, Yang JH, Zhang N, Huang T, Chen C (2012) J Mater Chem 22: 22398–22404
54. Huang JR, Mao C, Zhu YT, Jiang W, Yang XD (2014) Carbon 73:267–274
55. Maiti S, Suin S, Shrivastava N, Khatua BB (2014) RSC Adv 4:7979–7990
56. Gao JF, Li ZM, Peng S, Yan DX (2009) Polym Plast Tech Eng 48:478–481
57. Zeng Y, Lu GX, Wang H, Du JH, Ying Z, Liu C (2014) Sci Rep 4:6684
58. Du J, Zhao L, Zeng Y, Zhang L, Li F, Liu P, Liu C (2011) Carbon 49:1094–1100
59. Pang H, Zhang YC, Chen T, Zeng BQ, Li ZM (2010) Appl Phys Lett 96:251907
60. Ryu SH, Kim S, Kim H, Kang SO, Choa YH (2015) RSC Adv 5:36456
61. Thommerel ME, Valmalette JC, Musso J (2002) Mater Sci Eng A328:67–79
62. Tavman IH (1997) Powder Tech 91(1):63–67
63. Rusu M, Sofiana N, Rusu D (2001) Polym Test 20(4):409–417
64. Mamunya YP, Davydenko VV, Pissis P, Lebedev V (2002) Europ Polym J 38(9):1887–1897
65. Andrzej R, Gisele B, Flavien M, Gerard S (2010) Comp Sci Tech 70:410–416
66. Mitsuhiro K, Toru M (2005) Electr Eng Japan 2:1–9 (Translated from Denki Gakkai Ronbunshi, Vol. 124-A, No. 4, April 2004, pp 337–343
67. Sun Y, Bao HD, Guo ZX, Yu J (2009) Macromolecules 42:459–463
68. Zhang SM, Lin L, Deng H, Gao X, Bilotti E, Peijs T, Zhang Q (2012) Exp Polym Lett 6:159–168
69. Otten RHJ, Van DSP (2009) Phys Rev Lett 103:225704/1-4
70. Ma PC, Liu MY, Zhang H, Wang SQ, Wang R, Wang K, Wong YK, Tang BZ, Hong SH, Paik KW, Kim JK (2009) ACS Appl Mater Interfaces 1:1090–1096
71. Sumfleth J, Adroher XC, Schulte K (2009) J Mater Sci 44:3241–3247
72. Deng H, Lin L, Ji MZ, Zhang SM, Yang MB, Fu Q (2014) Prog Polym Sci 39:627–655
73. Zha JW, Li WK, Liao RJ, Bai J, Dang ZM, Mater J (2013) Chem A 1:843–851
74. Chekanov Y, Ohnogi R, Asai S (1999) J Mater Sci 34:5589–5592
75. Xue QZ (2004) Eur Polym J 40:323–327
76. Zhang C, Yi XS, Yui H, Asai S, Sumita M, Appl J (1998) Polym Sci 69(9):1813–1819
77. Xu HP, Dang ZM, Jiang MJ, Yao SH, Bai JB (2008) J Mater Chem 18:229–234
78. Dang ZM, Wang HY, XU HP (2006) Appl Phys Lett 89:112902

79. Bai BC, Kang SC, Im JS, Lee SH, Lee YS (2011) Mater Res Bull 46:1391–1397
80. He LX, Tjong SC (2015) RSC Adv 5:15070
81. Jia SJ, Jiang PK, Zhang ZC et al (2006) Effect of carbon-black treatment by radiation emulsion polymerization on temperature dependence of resistivity of carbon-black-filled polymer blends. Radiat Phys Chem 75:524–531
82. Michael S, Martin B, Jurgen H, Eur J (2005) Ceramic Soc 25:199–204
83. Chen JH, Wei G, Maekawa Y, Yoshida M, Tsubokawa N (2003) Polymer 44(11):3201–3207
84. Yang GC (1997) Polym Comp 18(4):484–491
85. Narkis M, Ram A, Stein Z (1981) Polym Eng Sci 21:1049–1054
86. Narkis M, Vaxman A (1984) J Appl Polym Sci 29:1639–1652
87. Zhang GX, Zhang ZC (2004) Radiat Phys Chem 71(1–2):273–276
88. Yi XS, Zhang JF, Zheng Q, Pan Y, Appl J (2000) Polym Sci 77(3):494–499
89. Seo MK, Rhee KY, Park SJ (2011) Curr Appl Phys 11:428–433
90. Chen JH, Iwata H, Tsubokawa N, Maekawa Y, Yoshida M (2002) Polymer 43(8):2201–2206
91. Hirano S, Kishimoto A (1998) Appl Phys Lett 73:25–27